

*Research article*

## **Modeling of stress distribution on the basis of the measured values of strain and temperature changes**

**Ivan Jandrlić<sup>1,\*</sup>, Stoja Rešković<sup>1</sup>, Dušan Ćurčija<sup>2</sup>, Ladislav Lazić<sup>1</sup> and Tin Brlić<sup>1</sup>**

<sup>1</sup> University of Zagreb Faculty of Metallurgy, Aleja narodnih heroja 3 Sisak, Croatia

<sup>2</sup> Croatian Metallurgical Society, Berislavićeva 6, 10000 Zagreb, Croatia

\* **Correspondence:** Email: [ijandrli@simet.hr](mailto:ijandrli@simet.hr); Tel: +38544533380.

**Abstract:** This paper proposes a new mathematical model for calculation of stresses on the basis of experimentally measured values of strains and temperature changes for niobium microalloyed steel. Construction of model was done using a multiple regression analysis of the measured values of temperature change, deformation and stresses at four different stretching rates. All investigations were conducted on samples from the niobium microalloyed steel, using thermography and digital image correlation during static tensile testing. Constructed model was tested and validated on the experimentally obtained results. Model showed a good agreement of calculated stress values with experimentally obtained ones.

**Keywords:** stress; temperature change; strain; mathematical model; stretching rate

---

### **1. Introduction**

To keep pace with today's rapid development in construction and production technology, engineers need to be able to quickly adapt to new types of materials. Engineers should conduct extensive materials testing to maintain the reliability of the built-in components. It is desired to minimize two required factors (time and money) in production. For this reason, engineers and researchers are turning to the modeling and increasingly use models based on the finite element

method [1–4]. Depending on what is wanted to be examined, models can be especially complex, as in the case of modeling of mechanical behavior of metal components that are under complex load.

During modeling, it is impossible to count all influencing parameters, so developed models always have some limitation. It is required to determine a significant number of parameters of material, for accurately simulation of real behavior of a certain component [3–6]. Linear regression is usually used to determine the interdependences of various parameters during modeling. Tikhonov-Morozov regularization is one of the most classic and important regularization method that has been efficiently utilized in literature to reduce the influence of measurement noise without notably distorting the measured data [7,8].

Researchers develop various models, ranging from modeling of some parameter behavior up to more complex ones for determining the material flow and stress distribution during loading [9–11]. Lately, there are new approaches in modeling of material flow by using digital image correlation (DIC). DIC method is mainly used for displacement and deformation analysis during deformation of materials [12–13]. Researchers can obtain a reliable data for construction of models on material flow with this method. It is so developed that it is even used to validate some developed models [13]. DIC method is fully optical, non-contact method and it is insensitive on the shape of the sample, what is one of its advantages.

Thermography is another method that is becoming more and more frequently used. This method is based on the premises that during the plastic deformation of the metals exists change in the internal energy of the deformed metal, which is manifested as the temperature change on the surface of sample in the deformation zone [14–16]. This change can be detected and measured by an infrared camera, and subsequent thermal analysis provides of the temperature distribution [12,16].

Clear insight on the metal flow, throughout the deformation zone, can be obtained from data achieved with thermography and DIC method [17]. During the analysis of results from DIC and thermography, the idea for a different and perhaps simpler approach to the modeling has emerged. The aim of this paper is to formulate a mathematical model, which can calculate the values of acting stresses from experimentally measured temperature changes, deformations and knowing stretching rates during tensile testing. The model will be formulated on the basis of experimentally determined values of deformation and temperature changes detected by the methods of digital image correlation and thermography. Once formulated, the model will be validated and verified by experimentally measured values.

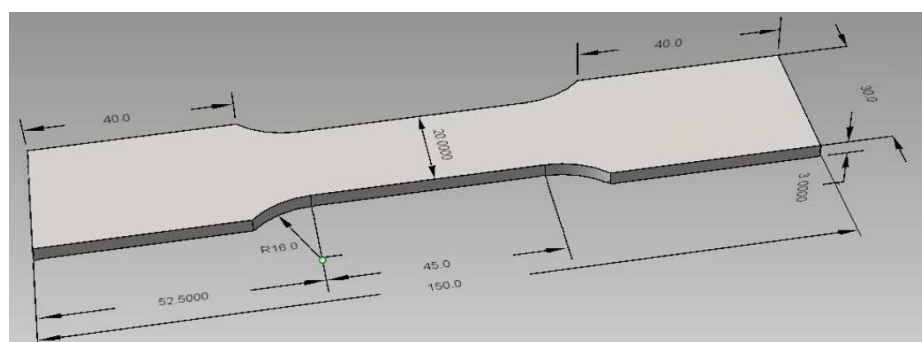
## **2. Materials and methods**

To determine the stresses, strains and temperature changes in the deformation zone during the static tensile testing the deformation of samples were recorded with an infrared and optical digital camera. Subsequent analysis of recorded data was done using thermography and digital image correlation method in order to determine the maximum values of temperature changes and strains. The maximum stresses were determined from static tensile testing in the same points. The chemical composition of the tested steel is given in Table 1.

**Table 1.** Chemical composition of the tested steel, wt%.

Element	C	Mn	Si	P	S	Al	Nb	N
Micro-alloyed steel	0.12	0.78	0.18	0.011	0.018	0.02	0.048	0.008

Tests were performed at four different stretching rates in range from 5 up to 30 mm min<sup>-1</sup>. The samples for static tensile testing were taken in rolling direction from 3 mm thick hot-rolled strip. Tests were performed on samples with rectangular cross-section, with gage length of 45 mm and gage width of 20 mm (Figure 1).

**Figure 1.** Configuration of the samples for tensile testing.

Using the MathCAD and OriginPro software packages, the analysis of variance-ANOVA and  $\chi^2$  test was performed on values of measured results. Subsequently, the multiple linear regression analysis was used to formulate the mathematical model for stress calculation.

### 3. Results and discussion

In the previous work [18], it was found out that stretching rate has influence on the measured values of temperature change, strain and stress. For that reason, the first step before formulating the model was to investigate interdependence of measured values at used stretching rates. The results of analysis on the influence of temperature change on the strain at all stretching rates are shown in Figure 2.

Analysis shows that in the case of microalloyed steel with the 0.048% of Nb, the temperature change increases with strain increase at all stretching rates. The increase in temperature is linear with strain increase. Linear equations, for the dependence between temperature change and strains, were determined for each stretching rate:

$$v_1 \rightarrow \Delta T = 87.012 \cdot \varepsilon - 0.745 \quad (1)$$

$$v_2 \rightarrow \Delta T = 117.0 \cdot \varepsilon - 1.275 \quad (2)$$

$$v_3 \rightarrow \Delta T = 135.84 \cdot \varepsilon - 1.69 \quad (3)$$

$$v_4 \rightarrow \Delta T = 160.06 \cdot \varepsilon - 3.1 \quad (4)$$

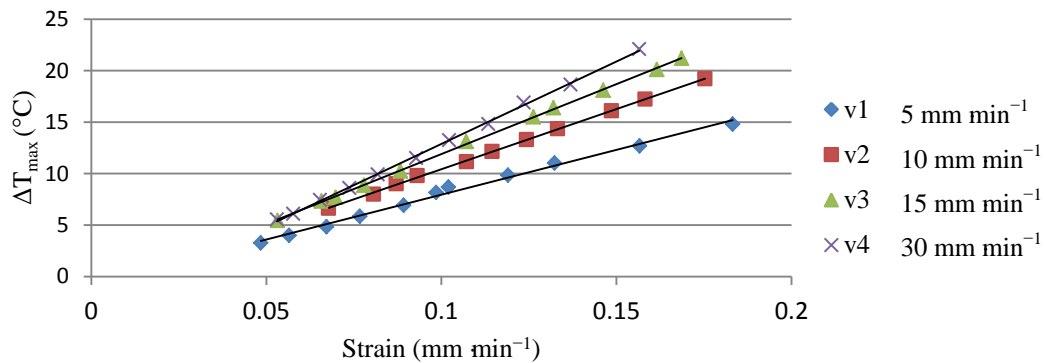


**Figure 2.** Influence of stretching rate on the dependence between temperature change and strain.

It is clear that temperature change increase is even more pronounced by increasing the stretching rate from obtained dependences and equations. So this needs to be taken into account when formulating mathematical model. This indicates a close relationship between deformation (i.e., strain), stretching rate (i.e., strain rate) and temperature changes. In order to clarify the influence of stress on the temperature change, analyses were done on relationship between stress and temperature change at all used stretching rates (Figure 3).

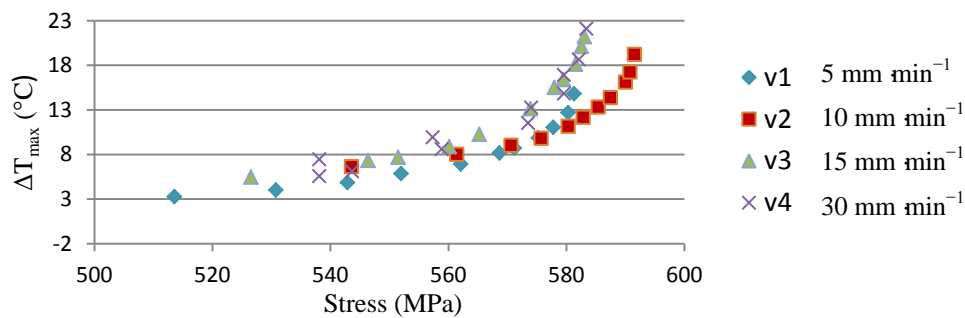


**Figure 3.** Influence of stretching rate on the dependence between stress and temperature change.

It is a reasonable assumption the maximum stresses are acting where maximum temperature change occurs at the place of the maximum deformation. Starting from this assumption, the stress values were determined from results of the tensile test. At the same points where the values of temperature change and strain were determined from thermography and DIC, the stress values were read out from the results of the tensile test. As can be seen in the above correlation diagram, the increase in stress has a significant effect on the temperature change. Influence of stretching rate is not so much pronounced as in the case of relation  $\Delta T_{\max} - \varepsilon$ , but it is still present. There is a higher

temperature change increase by increasing stretching rate. Functional relationship between temperature change and stresses is represented by an exponential function at all used stretching rate.

From obtained dependencies in Figures 2 and 3, one can conclude that the measured temperature changes are closely related to the stretching rate, values of stress and strains achieved during the tensile test. Accordingly, the following relation can be set:

$$\Delta T = f(\sigma, \varepsilon, \nu) \quad (5)$$

where is:  $\sigma$ —stress (MPa)

$\varepsilon$ —strain ( $\text{mm mm}^{-1}$ )

$\nu$ —stretching rate ( $\text{mm mm}^{-1}$ )

By the further transformation of Eq 5, stress can be determined from measured values of temperature changes, strains and known stretching rate:

$$\sigma = f(\Delta T, \varepsilon, \nu) \quad (6)$$

The functional relationships between the temperature changes, strains, stress and stretching rates was formulated using the multiple linear regression analysis. At first the multiple linear regressions was carried out on the experimentally obtained results from thermography, static tensile test and digital image correlation, at each stretching rate separately.

$$\nu_1 = 5 \text{ mm} \cdot \text{min}^{-1} \rightarrow \Delta T = 1.1 + 92.1 \cdot \varepsilon - 0.0037 \cdot \sigma \quad (7)$$

$$\nu_2 = 10 \text{ mm} \cdot \text{min}^{-1} \rightarrow \Delta T = 1.6 + 140.2 \cdot \varepsilon - 0.0077 \cdot \sigma \quad (8)$$

$$\nu_3 = 15 \text{ mm} \cdot \text{min}^{-1} \rightarrow \Delta T = 2.0 + 157.2 \cdot \varepsilon - 0.0104 \cdot \sigma \quad (9)$$

$$\nu_4 = 30 \text{ mm} \cdot \text{min}^{-1} \rightarrow \Delta T = 3.1 + 210.0 \cdot \varepsilon - 0.0210 \cdot \sigma \quad (10)$$

The general function of dependency of temperature change on the strain and corresponding stresses is in the form of:

$$\Delta T = a + b \cdot \varepsilon + c \cdot \sigma \quad (11)$$

where is:  $a, b, c$ —parameters dependent on stretching rate.

It is clear that by increasing stretching rate, there is the change in the values of the determined parameters  $a, b$ , and  $c$  (Table 2).

**Table 2.** Determined values of parameter  $a, b$ , and  $c$  at different stretching rates for Nb microalloyed steel.

Stretching rate ( $\text{mm min}^{-1}$ )	a	b	c
5	1.1	92.1	-0.0037
10	1.6	140.2	-0.0077
15	2.0	157.2	-0.0104
30	3.1	210.0	-0.0210

Functional dependency of parameters on the stretching rate is shown by Figure 4. Dependences of parameters  $a$ ,  $b$  and  $c$  on the stretching rate is given by following relations:

$$a = 0.4305 \cdot v^{0.5758} \quad (12)$$

$$b = 46.364 \cdot v^{0.4515} \quad (13)$$

$$c = -0.007 \cdot v \quad (14)$$

By incorporating functional dependences of parameters  $a$ ,  $b$  and  $c$  as a function of stretching rate in the initial Eq 11, obtained by linear regression, the function of temperature change is now:

$$\Delta T = 0.4305 \cdot v^{0.5758} + 46.364 \cdot v^{0.4515} \cdot \varepsilon - 0.007v \cdot \sigma \quad (15)$$

By transformation of Eq 15 it is possible to express the stress as the function of temperature change, strains and stretching rate:

$$\sigma = \frac{0.4305 \cdot v^{0.5758} + 46.364 \cdot v^{0.4515} \cdot \varepsilon - \Delta T}{0.007v} \quad (16)$$

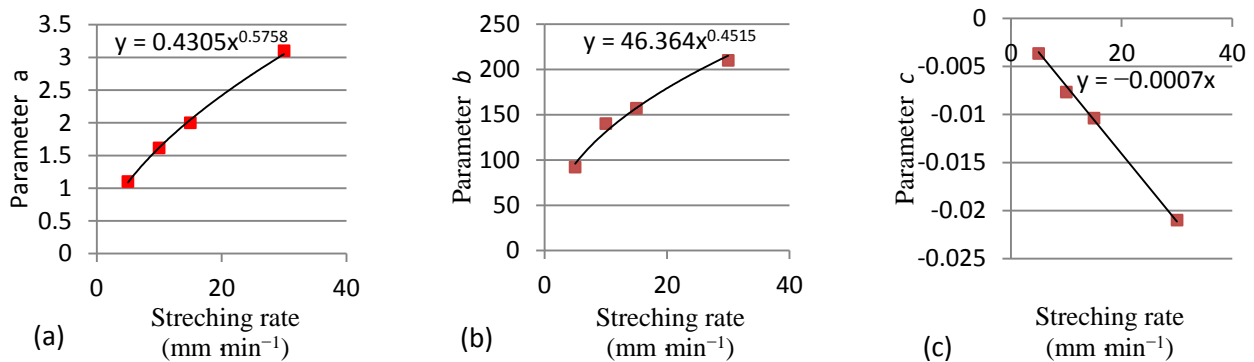


**Figure 4.** Dependency of function parameters on the testing speed.

The mathematical model for stress calculation formulated on the basis of the above achieved regression equations was validated and verified with the measured values of strains and temperature changes at all used stretching rates. The comparison between the model and the experimentally measured values is shown in Figure 5.

As it can be seen from given diagrams, it has been achieved a good agreement between model and experimentally measured values up to the stretching rate of 30 mm min<sup>-1</sup>. Some deviations of modeled values can be observed at 5 mm min<sup>-1</sup>. This is only in the beginning of plastic flow, and afterwards there is a good agreement between modeled and measured values.

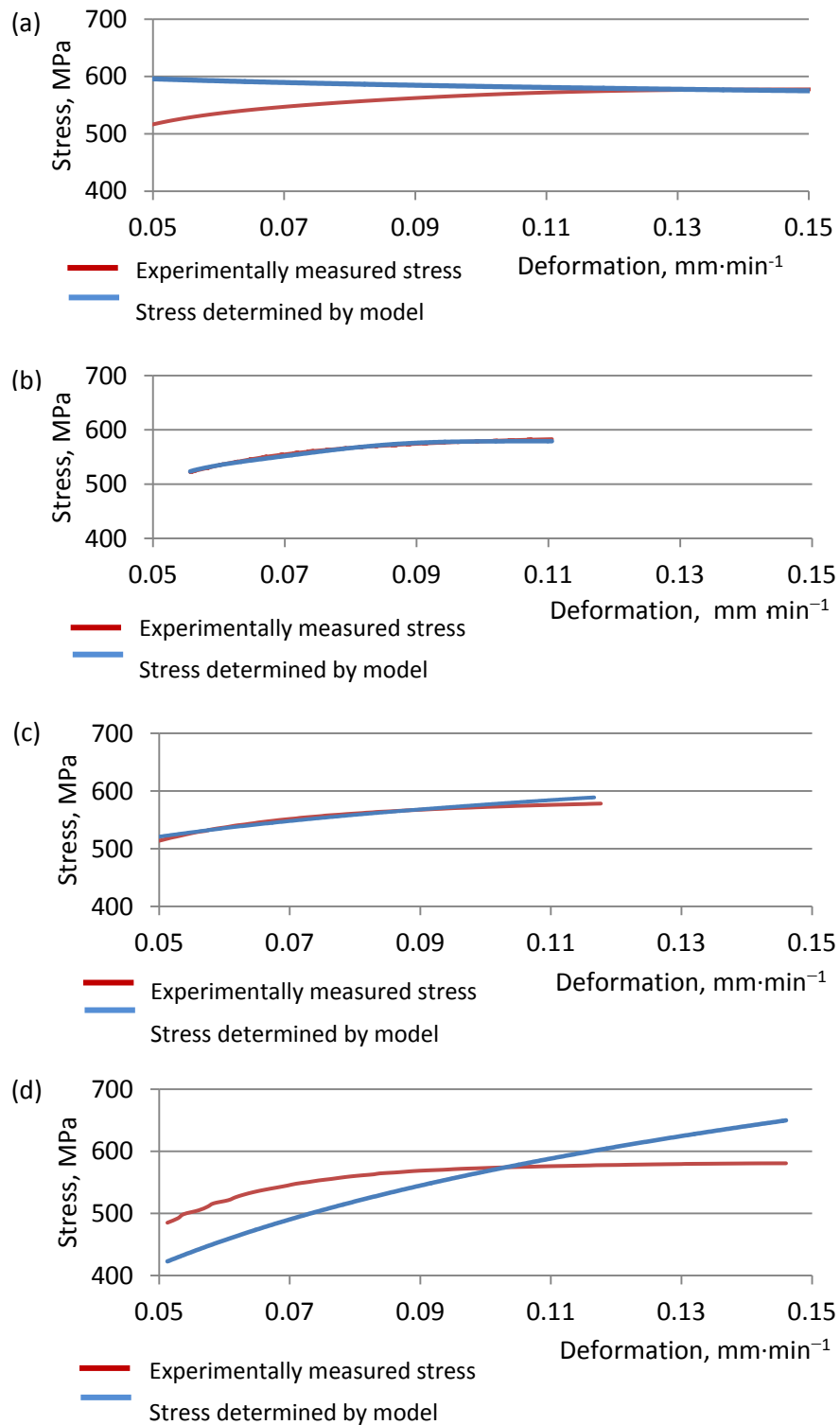


**Figure 5.** Comparison between the calculated values and the experimentally measured values. Testing speed: (a) 5 mm min<sup>-1</sup>, (b) 10 mm min<sup>-1</sup>, (c) 15 mm min<sup>-1</sup> and (d) 30 mm min<sup>-1</sup>.

#### 4. Conclusions

ANOVA and  $\chi^2$  test analysis conducted on experimentally obtained data established that there is strong interdependence between measured values of temperature changes, strain, stresses and stretching rate during deformation of the tested samples. The functional relationship was determined using multiple linear regression analysis between the three independent variables temperature changes, stretching rate and strains and the stresses as the dependent variable.

Formulated mathematical model enables the calculation of acting stresses in the deformation zone on the basis of the experimentally measured values of temperature changes, strains and known used stretching rate. Model was validated and verified by comparing the calculated and experimentally determined values. Model accurately calculated stress values on the basis of measured values of temperature change and deformation up to the stretching rate of  $30 \text{ mm min}^{-1}$ .

#### Acknowledgements

This work has been fully supported by the Croatian Science Foundation under the project number IP-2016-06-1270.

#### Conflict of interests

All authors declare no conflicts of interest in this paper.

#### References

1. Seif M, Main J, Weigand J, et al. (2016) Finite element modeling of structural steel component failure at elevated temperatures. *Structures* 6: 134–145.
2. Lambiase F, Di Ilio A (2013) Finite element analysis of material flow in mechanical clinching with extensible dies. *J Mater Eng Perform* 22: 1629–1636.
3. Lee HW, Han JY, Kang JH (2016) A study on high speed coupling design for wind turbine using a finite element analysis. *J Mech Sci Technol* 30: 3713–3718.
4. Izadpanah S, Ghaderi SH, Gerdooei M (2016) Material parameters identification procedure for BBC2003 yield criterion and earing prediction in deep drawing. *Int J Mech Sci* 115: 552–563.
5. Li C, Daxin E, Yi N (2016) Analysis on fracture initiation and fracture angle in ductile sheet metal under uniaxial tension by experiments and finite element simulations. *J Mater Res* 31: 3991–3999.
6. Gu SH (2017) Application of finite element method in mechanical design of automotive parts. *IOP Conf Ser Mater Sci Eng* 231: 012180.
7. Faghidian SA (2014) A smoothed inverse eigenstrain method for reconstruction of the regularized residual fields. *Int J Solids Struct* 51: 4427–4434.
8. Faghidian SA (2016) A regularized approach to linear regression of fatigue life measurements. *Int J Struct Integrity* 7: 95–105.

9. Abspoel M, Scholting ME, Lansbergen M, et al. (2017) A new method for predicting advanced yield criteria input parameters from mechanical properties. *J Mater Process Tech* 248: 161–177.
10. Yang TS, Chang SY (2012) Investigation into the extrusion of porous metal using finite element method. *T Famena* 36: 13–22.
11. Merklein M, Biasutti M (2016) Development of a biaxial tensile machine for characterization of sheet metals. *J Mater Process Tech* 213: 939–946.
12. Jandrlic I, Reskovic S, Brlic T (2018) Distribution of stress in deformation zone of niobium microalloyed steel. *Met Mater Int* 24: 746–751.
13. Eskandari M, Zarei-Hanzaki A, Yadegari M, et al. (2014) In situ identification of elastic-plastic strain distribution in a microalloyed transformation induced plasticity steel using digital image correlation. *Opt Laser Eng* 54: 79–87.
14. Lava P, Cooreman S, Debruyne D (2010) Study of systematic errors in strain fields obtained via DIC using heterogeneous deformation generated by plastic FEA. *Opt Laser Eng* 48: 457–468.
15. Rusinek A, Klepaczko JR (2009) Experiments on heat generated during plastic deformation and stored energy for TRIP steels. *Mater Design* 30: 35–48.
16. Kutin MM, Ristic SS, Prvulovic MR, et al. (2011) Application of thermography during tensile testing of butt welded joints. *FME T* 39: 133–138.
17. Ryu JH, Kim JI, Kim HS, et al. (2013) Austenite stability and heterogeneous deformation in fine-grained transformation-induced plasticity assisted steel. *Scripta Mater* 68: 933–936.
18. Jandrlic I (2015) The stress distribution in the deformation zone of niobium microalloyed steel [PhD's thesis]. University of Zagreb Faculty, Croatia.



AIMS Press

© 2019 the Author(s), licensee AIMS Press. This is an open access article distributed under the terms of the Creative Commons Attribution License (<http://creativecommons.org/licenses/by/4.0>)